

## Robust Fault Detection Method for Uncertain Multivariable Systems with Application to Twin Rotor MIMO System

金 臺祐 · 俞 浩濬 · 權 五圭

(Dae-Woo Kim · Ho-Jun Yoo · Oh-Kyu Kwon)

**Abstract** - This paper deals with the fault detection problem in uncertain linear multivariable systems and its application. A robust fault detection method presented by Kim et al. (1998) for MIMO (Multi Input/Multi Output) systems has been adopted and applied to the twin rotor MIMO experimental setup using industrial DSP. The system identification problem is formulated for the twin rotor MIMO system and its parameters are estimated using experimental data. Based on the estimated parameters, some fault detection simulations are performed using the robust fault detection method, which shows that the performance is satisfied.

**Key Words** : Fault detection; multivariable system; parameter estimation; MIMO application; linearization errors; bias errors; variance errors.

## 1. Introduction

Most of FDI (Fault Detection and Isolation) method using analytical redundancy are based on a number of idealized assumptions. Any method developed in the idealized assumptions works only if the adopted system models exactly represents the monitored physical system and no noise or unexpected disturbances are presented. In practice, these requirements are rather stringent and are met in few real systems. Usually, the parameters of the system are uncertain or varying with time, and the characteristics of the disturbances and noise are unknown so that there is always a mismatch between the actual process and its mathematical model even if no fault occurs in the process. Since the model mismatch causes performance degradation and false alarm, the effect of model uncertainties is one of the most crucial point in FDI.

To overcome this difficulty, the FDI algorithm has to be made robust to the model uncertainty. The robustness problem has already become an issue of the area of fault

detection and diagnosis. Many authors (e. g., Basseville, 1988; Lou *et al.*, 1986; Ninness *et al.*, 1991; Patton and Chen, 1993) refer to the importance of this problem, and several methods are proposed to improve the robustness to modelling errors, noises and disturbances in the fault detection and diagnosis. See, for example, Isermann (1993), Kwon *et al.* (1994), Howell(1994), Frank (1995) and Chen *et al.* (1996). However, most of them are based on SISO (Single Input/Single Output) systems.

Linear controllers such as PID or phase lead, lag are widely used in real industrial fields because they are simple and has robust characteristic. But these methods are could be adopted in SISO system or we must derive the decoupled system. Nevertheless it is not satisfied that robustness for the modelling error and disturbance in MIMO system. LQG/LTR technique, which was proposed in early of 1980, has advantages of multivariable systems design.

The key aspects in this paper is to verify the performance of the robust fault detection method for MIMO (Multi Input/Multi Output) system proposed by Kim *et al.* (1998). The robust fault detection method is implemented in this paper by using industrial DSP (Digital Signal Processing) board and applied to a twin rotor MIMO experimental setup which is controlled by LQG/LTR control technique.

\* 正 會 員 : 仁荷大 工大 電氣工學科 博士課程

\*\* 正 會 員 : 仁荷大 工大 電氣工學科 教授 · 工博

接受日字 : 1998年 6月 5日

最終完了 : 1999年 1月 11日

Because the controlled system is highly nonlinear and coupled, so it is very difficult to derive the exact model of the system. Even though the system model is not correct, the robust fault detection algorithm will work and show good result for the small change of system parameter. In practice, two sources of error, undermodelling and noise, are likely to be of comparable significance and both need to be accounted in the design of an appropriate fault detection procedure.

The layout of the paper is as follows: In Section 2, the system description and the robust fault detection method are summarized in linear MIMO systems with undermodelling and noise. Section 3 the target system is described and the model is identified. In Section 4, the experimental procedure, is described, and experimental results and conclusions are given.

## 2. Robust Fault Detection Method

### 2.1 System Description

One way of representing the model mismatch is to incorporate additive unmodelled dynamics into the system description as shown in Fig. 1.

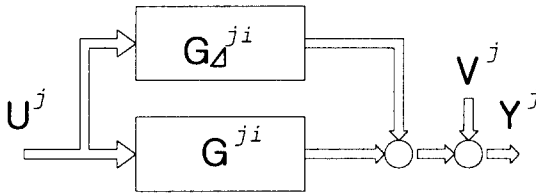


Fig 1. System with the unmodelled dynamics

It is assumed that the true system  $G_T$  and the nominal model  $G$  are stable and causal discrete-time systems. For simplicity, in this paper, the nominal model from the  $i$  th input to the  $j$  th output is taken to be of the form

$$G_{ji}(z^{-1}, \theta^i) = \frac{B_{ji}(z^{-1}, \theta^i, N_B^i)}{F_{ji}(z^{-1}, N_F^i)} \quad (1)$$

$$i = 1, 2, 3, \dots, m, \quad j = 1, 2, \dots, q$$

where  $z$  is the discrete transform variable,  $F_{ji}(z^{-1}, N_F^i)$  is a predetermined denominator and

$$B_{ji}(z^{-1}, \theta^i, N_B^i) \equiv b_1^i z^{-1} + b_2^i z^{-2} + \dots + b_{N_B^i}^i z^{-N_B^i}$$

$$F_{ji}(z^{-1}, N_F^i) \equiv 1 + f_1^i z^{-1} + f_2^i z^{-2} + \dots + f_{N_F^i}^i z^{-N_F^i}$$

$$\theta^i \equiv [b_1^i \ b_2^i \ \dots \ b_{N_B^i}^i]^T$$

Note that any linear stable system can be approximated by the nominal model (1) by adjusting the orders  $N_B^i$  and  $N_F^i$  (Salgado, 1989). FIR models and the Laguerre models studied by Makila (1990) and Wahlberg (1991) are examples of such a model structure. The advantage of representation (1) is that it allows the nominal impulse response to be represented by a linear function of the system parameters, and this facilitates parameter estimation and the quantification of the effects of the bias error on the estimated model.

Using the system description of Fig. 1, the  $j$ th system output can be represented as follows:

$$y^j(k) = \sum_{i=1}^m G_{Tji}(q^{-1}) u^i(k) + v^j(k)$$

$$= \sum_{i=1}^m B_{ji}(q^{-1}, \theta^i, N_B^i) u_F^i(k) + \sum_{i=1}^m G_{\Delta ji}(q^{-1}) u^i(k) + v^j(k) \quad (2)$$

where  $q^{-1}$  denotes the backward shift operator and

$$u_F^i(k) \equiv \frac{1}{F_{ji}(q^{-1}, N_F^i)} u^i(k).$$

Denoting the impulse response of  $G_{\Delta ji}$  by  $h^i(\cdot)$ , and assuming that  $u^i(k) = 0$  for  $k \leq 0$  and  $h^i(\cdot)$  has the finite duration  $N_h^i$ . Equation (2) can be rewritten compactly as follows:

$$Y^j = \Phi^j \Theta^j + \Psi^j H^j + V^j \quad (3)$$

For simplicity, it is assumed that  $v^j(\cdot)$  is a white noise sequence having variance  $\sigma^2$ . The nominal parameter vector  $\Theta^j$  can be estimated by the ordinary linear least-squares method as follows:

$$\hat{\Theta}^j = [(\Phi^j)^T \Phi^j]^{-1} (\Phi^j)^T Y^j \quad (4)$$

The main interest here is to quantify the effect of the noise  $V^j$  and undermodelling  $\Psi^j H^j$  in (3) on the estimate  $\hat{\Theta}^j$  of (4). Substituting (3) into (4) gives

$$\hat{\Theta}^j - \Theta^j = [(\Phi^j)^T \Phi^j]^{-1} (\Phi^j)^T [\Psi^j H^j + V^j] \quad (5)$$

$$= \tilde{\Theta}_1^j + \tilde{\Theta}_2^j \quad (6)$$

where  $\tilde{\Theta}_1^j$  and  $\tilde{\Theta}_2^j$  are called the variance and bias errors, respectively, and they are defined by

$$\tilde{\Theta}_1^j \equiv [(\Phi^j)^T \Phi^j]^{-1} (\Phi^j)^T V^j \quad (7)$$

$$\tilde{\Theta}_2^j \equiv [(\Phi^j)^T \Phi^j]^{-1} (\Phi^j)^T \Psi^j H^j \quad (8)$$

### 2.2 Bias and Variance Error Evaluation

The fault detection procedure to be described below depends on using a measure of the total error in the parameter estimates due to noise and undermodelling. In this section, firstly, the variance error due to noise will be considered, and, secondly, the bias error due to undermodelling will be examined.

In the model of Section 2, the regression vectors  $\Phi^j$  and  $\Psi^j$  are functions of only the input. Hence the covariance of the variance error  $E[\tilde{\Theta}_1^j (\tilde{\Theta}_1^j)^T]$  can be evaluated directly from (7) as

$$E[\tilde{\Theta}_1^j (\tilde{\Theta}_1^j)^T] = [(\Phi^j)^T \Phi^j]^{-1} \sigma^2 \quad (9)$$

where  $\sigma^2$  is the variance of the measurement noise  $\nu(\cdot)$ . Hereafter,  $\sigma^2$  is assumed to be known. Clearly, from (8), to be able to say something about the size of the bias error, it is necessary to know something about  $H^j$ .

If prior information about the likely undermodelling is not available, then  $H^j$  can be estimated from the available data. Note that this additional estimate is used only in the quantification of the likely errors in  $\hat{\Theta}^j$  due to  $H^j$  and not in building a more complex model. An obvious estimate of  $H^j$  is to use the full model, *i.e.*, from (3)

$$\begin{bmatrix} \hat{\Theta}^j_{FULL} \\ \hat{H}^j \end{bmatrix} = \begin{bmatrix} (\Phi^j)^T \Phi^j & (\Phi^j)^T \Psi^j \\ (\Psi^j)^T \Phi^j & (\Psi^j)^T \Psi^j \end{bmatrix}^{-1} \begin{bmatrix} (\Phi^j)^T \\ (\Psi^j)^T \end{bmatrix} Y^j$$

Thus the inversion formula for a partitioned matrix gives

$$\hat{H}^j = [(\Psi^j)^T \Pi^j \Psi^j]^{-1} (\Psi^j)^T \Pi^j Y^j$$

where  $\Pi^j \equiv I - \Phi^j [(\Phi^j)^T \Phi^j]^{-1} (\Phi^j)^T$

and we have

$$E[(\hat{H}^j - H^j)(\hat{H}^j - H^j)^T] = [(\Psi^j)^T \Pi^j \Psi^j]^{-1} \sigma^2. \quad (10)$$

To evaluate the expected size of  $H^j$ , a Bayesian

embedding argument is invoked. If  $H^j$  is considered as a realization of a random variable, provided the noise is gaussian, then  $\hat{H}^j$  and  $[(\Psi^j)^T \Pi^j \Psi^j]^{-1} \sigma^2$  can be viewed as the *a posteriori* mean and covariance of the conditional distribution for  $H^j$ , given the data  $Y^j$ . Under these conditions, from (10),

$$\begin{aligned} E[H^j(H^j)^T | Y^j] &= E[(\hat{H}^j - \hat{H}^j + H^j)(\hat{H}^j - \hat{H}^j + H^j)^T | Y^j] \\ &= \hat{H}^j(\hat{H}^j)^T + [(\Psi^j)^T \Pi^j \Psi^j]^{-1} \sigma^2 \equiv C^j_{ho} \end{aligned} \quad (11)$$

Thus, from (8),

$$\begin{aligned} E[\tilde{\Theta}_2^j (\tilde{\Theta}_2^j)^T | Y^j] &= \\ &= [(\Phi^j)^T \Phi^j]^{-1} (\Phi^j)^T \Psi^j C^j_{ho} (\Psi^j)^T \Phi^j [(\Phi^j)^T \Phi^j]^{-1} \end{aligned}$$

Provided an independent data set is used to estimate  $C^j_{ho}$ , then the total error covariance can be represented by the summing form with variance. Thus, in the sequel, the common symbol  $C^j_h$  will be used to denote either  $C^j_{ho}$  (when *a priori* data about  $H^j$  is used) or  $C^j_{ha}$  (when *a posteriori* data about  $H^j$  is used).

### 2.3 Fault Detection Method

The bias and variance errors have been expressed by the results of the previous two sections. These give the basis of the fault detection method to be proposed. Suppose that there are two sets of data  $I^j_n = \{Y^j_n, (\Phi^j)_n, (\Psi^j)_n\}$  and  $I^j_f = \{Y^j_f, (\Phi^j)_f, (\Psi^j)_f\}$ , which correspond to nonfaulty and faulty systems, respectively. The data is assumed to be modelled analogously to (3) as

$$Y^j_n = (\Phi^j)_n \Theta^j_n + (\Psi^j)_n H^j_n + V^j_n \quad (12)$$

$$Y^j_f = (\Phi^j)_f \Theta^j_f + (\Psi^j)_f H^j_f + V^j_f \quad (13)$$

Given  $I^j_n$  and  $I^j_f$ , the objective is to determine whether or not a fault has occurred in the second set of data  $I^j_f$ .  $\Theta^j_n$  and  $\Theta^j_f$  are estimated by the least-squares method as follows:

$$\begin{aligned} \hat{\Theta}^j_n &= [(\Phi^j)_n^T (\Phi^j)_n]^{-1} (\Phi^j)_n^T Y^j_n \\ \hat{\Theta}^j_f &= [(\Phi^j)_f^T (\Phi^j)_f]^{-1} (\Phi^j)_f^T Y^j_f \end{aligned}$$

The basic idea of the fault detection procedure is to compare the observed change  $\hat{\Theta}^j_n - \hat{\Theta}^j_f$  with the

likely errors that can result from noise and undermodelling alone, *i.e.*, when no fault has occurred. If the observed change is greater than that which can be explained by these two effects, then it will be concluded that a fault has occurred.

The composite data of (12) and (13) can be written as

$$\begin{bmatrix} Y_n^j \\ Y_f^j \end{bmatrix} = \begin{bmatrix} (\Phi_n^j) & 0 \\ 0 & (\Phi_f^j) \end{bmatrix} \begin{bmatrix} \Theta_n^j \\ \Theta_f^j \end{bmatrix} + \begin{bmatrix} (\Psi_n^j) & 0 \\ 0 & (\Psi_f^j) \end{bmatrix} \begin{bmatrix} H_n^j \\ H_f^j \end{bmatrix} + \begin{bmatrix} V_n^j \\ V_f^j \end{bmatrix} \quad (14)$$

hence using the techniques of Section 3,

$$E \left\{ \begin{bmatrix} \widehat{\Theta}_{n1}^j \\ \widehat{\Theta}_{f1}^j \end{bmatrix} \begin{bmatrix} \widehat{\Theta}_{n1}^j \\ \widehat{\Theta}_{f1}^j \end{bmatrix}^T \right\} = \begin{bmatrix} [(\Phi_n^j)^T (\Phi_n^j)]^{-1} \sigma^2 & 0 \\ 0 & [(\Phi_f^j)^T (\Phi_f^j)]^{-1} \sigma^2 \end{bmatrix} \quad (15)$$

$$E \left\{ \begin{bmatrix} \widehat{\Theta}_{n2}^j \\ \widehat{\Theta}_{f2}^j \end{bmatrix} \begin{bmatrix} \widehat{\Theta}_{n2}^j \\ \widehat{\Theta}_{f2}^j \end{bmatrix}^T \right\} = \begin{bmatrix} \alpha & \beta \\ \beta^T & \gamma \end{bmatrix}, \quad (16)$$

where

$$\alpha = [(\Phi_n^j)^T \Phi_n^j]^{-1} (\Phi_n^j)^T \Psi_n^j C_{h1}^j (\Psi_n^j)^T \Phi_n^j [(\Phi_n^j)^T \Phi_n^j]^{-1}$$

$$\beta = [(\Phi_n^j)^T \Phi_n^j]^{-1} (\Phi_n^j)^T \Psi_n^j C_{h12}^j (\Psi_f^j)^T \Phi_f^j [(\Phi_f^j)^T \Phi_f^j]^{-1}$$

$$\gamma = [(\Phi_f^j)^T \Phi_f^j]^{-1} (\Phi_f^j)^T \Psi_f^j C_{h2}^j (\Psi_f^j)^T \Phi_f^j [(\Phi_f^j)^T \Phi_f^j]^{-1}$$

and

$$E \left\{ \begin{bmatrix} H_n^j \\ H_f^j \end{bmatrix} \begin{bmatrix} H_n^j \\ H_f^j \end{bmatrix}^T \right\} = \begin{bmatrix} C_{h1}^j & C_{h12}^j \\ (C_{h12}^j)^T & C_{h2}^j \end{bmatrix} \quad (17)$$

Since it is necessary to evaluate the expected size of  $\widehat{\Theta}_n^j - \widehat{\Theta}_f^j$  when no fault occurs, then this calculation should be carried out under the hypothesis that  $H_n^j = H_f^j$  in (12),(13), and (17), *i.e.*,

$$C_{h1}^j = C_{h12}^j = C_{h2}^j = C_h^j \quad (18)$$

**Lemma 1:** Under the hypothesis that no fault has occurred,

$$\begin{aligned} E [(\widehat{\Theta}_{n1}^j - \widehat{\Theta}_{f1}^j)(\widehat{\Theta}_{n1}^j - \widehat{\Theta}_{f1}^j)^T] \\ = [(\Phi_n^j)^T \Phi_n^j]^{-1} \sigma^2 + [(\Phi_f^j)^T \Phi_f^j]^{-1} \sigma^2 \end{aligned} \quad (19)$$

$$\begin{aligned} E [(\widehat{\Theta}_{n2}^j - \widehat{\Theta}_{f2}^j)(\widehat{\Theta}_{n2}^j - \widehat{\Theta}_{f2}^j)^T] \\ = (Q_n^j - Q_f^j) C_h^j (Q_n^j - Q_f^j)^T, \end{aligned} \quad (20)$$

where  $Q_n^j \equiv [(\Phi_n^j)^T (\Phi_n^j)]^{-1} (\Phi_n^j)^T (\Psi_n^j)$  (21)

$$Q_f^j \equiv [(\Phi_f^j)^T (\Phi_f^j)]^{-1} (\Phi_f^j)^T (\Psi_f^j) \quad (22)$$

Proof: Note that

$$\widehat{\Theta}_{ns}^j - \widehat{\Theta}_{fs}^j = [I - I] \begin{bmatrix} \widehat{\Theta}_{ns}^j \\ \widehat{\Theta}_{fs}^j \end{bmatrix}, \quad s = 1, 2.$$

The result then follows from (15) and (16) on using (18).  $\square$

**Remark 4.1:** An interesting fact, which follows from (20), is that if the two experiments are identical, then the expected value of the systematic error due to undermodelling is zero.  $\square$

**Remark 4.2:** The variance error (19) and the bias error (20) should be combined to evaluate the total error in  $\widehat{\Theta}_n^j - \widehat{\Theta}_f^j$ . In the model of Section 2, provided  $V$  and  $C_{ho}^j$  are independent, then there is no cross term, and hence

$$\begin{aligned} E [(\widehat{\Theta}_n^j - \widehat{\Theta}_f^j)(\widehat{\Theta}_n^j - \widehat{\Theta}_f^j)^T] = \\ [ [(\Phi_n^j)^T (\Phi_n^j)]^{-1} + [(\Phi_f^j)^T (\Phi_f^j)]^{-1} ] \sigma^2 \\ + (Q_n^j - Q_f^j) C_{ho}^j (Q_n^j - Q_f^j)^T \end{aligned} \quad (23)$$

This expression can be also used in a case where  $C_{ho}^j$  is replaced by  $C_{ha}^j$ . Note that this case, in principle, requires that an independent set of data be used to estimate  $C_{ha}^j$  as in (11).  $\square$

The fault detection method proposed will be based on simple functions of the covariance for the estimated parameter change  $\widehat{\Theta}_n^j - \widehat{\Theta}_f^j$  given in (23). A variety of functions could be employed. For illustration, the following simple quadratic function will be used:

$$T_1 \equiv (\widehat{\Theta}_n^j - \widehat{\Theta}_f^j)^T (C^j)^{-1} (\widehat{\Theta}_n^j - \widehat{\Theta}_f^j) \quad (24)$$

The test variable in (24) is based on the comparison between the estimate  $\widehat{\Theta}_n^j - \widehat{\Theta}_f^j$  and its covariance  $C^j$ . If the test variable is larger than a fixed threshold, this is taken as evidence that the system parameters have changed, *i.e.*, a fault has occurred. Note, in a case where noise alone is considered, that  $T_1$  is the standard  $\chi^2$  test variable (Willsky, 1976), and the threshold value can be determined from the confidence level consideration of the  $\chi^2$  table.

### 3. Twin Rotor MIMO Experimental Setup

#### 3.1 System drive

LQG/LTR is a well known controller synthesis method

of multivariable system with modelling error. To get a reliable loop configuration, which satisfies performance-robustness, we synthesis target filter loop using Kalman filter, and perform loop transfer recovery procedure using cheap linear controller. Block diagram of LQG/LTR controller is can be shown Fig 3.1 including system noise  $w$  and measurement noise  $v$ .

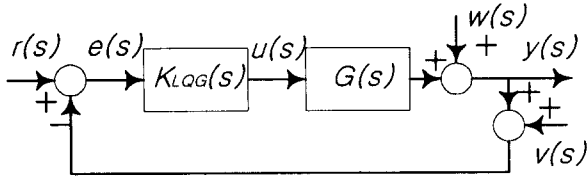


Fig 3.1 Block diagram of feedback controller

For reference tracking and zero steady state error , synthesis plant model can be made as equation (25) which include integral component.

$$\begin{aligned} \dot{x}(t) &= Ax(t) + Bu(t) \\ y(t) &= Cx(t) \end{aligned} \quad (25)$$

where

$$x(t) = \begin{bmatrix} u_p(t) \\ x_p(t) \end{bmatrix}, A = \begin{bmatrix} 0 & 0 \\ B_p & A_p \end{bmatrix}, B = \begin{bmatrix} I \\ 0 \end{bmatrix}, C = [0 \quad C_p]$$

and the subscript  $p$  means the plant variables. Required transfer function of target filter loop is (26) and structure is shown in Fig 3.2.

$$G_{KF}(s) = C(sI - A)^{-1}H \quad (26)$$

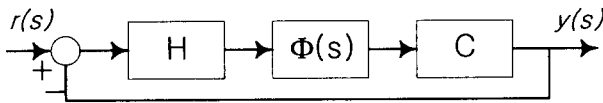


Fig 3.2 Target filter loop

The Kalman filter gain  $H$  is calculated by (27), and  $P$  is the solution of the Riccati equation (28).

$$H = \frac{1}{\mu} PC^T \quad (27)$$

$$0 = AP + PA^T + LL^T - \frac{1}{\mu} PC^T CP \quad (28)$$

where  $\mu$  is the synthesis coefficient which comes from the cross frequency ( $\omega_c$ ),

$$\mu = \frac{1}{\omega_c^2}$$

Choice of  $L$  which satisfies the singular value matching condition in low frequency and high frequency is shown by (29)

$$L = \begin{bmatrix} -(C_p A_p^{-1} B_p)^{-1} \\ C_p^T (C_p C_p^T)^{-1} \end{bmatrix} \quad (29)$$

where  $[A, B]$  is stabilizable, and  $[A, C]$  is detectable.

Loop recovery can be performed by such (30) and the structure can be shown in Fig 3.3

$$u(s) = K(s)_{LQG/LTR} e(s)$$

$$K(s)_{LQG/LTR} = G(sI - A + BG - HC)^{-1}H \quad (30)$$

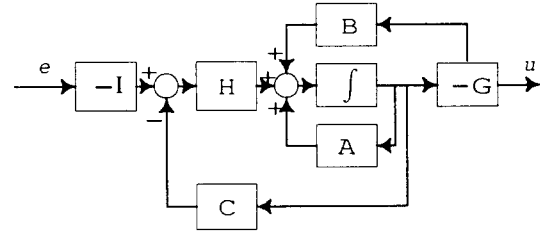


Fig 3.3 Block diagram of LQG/LTR controller

Control gain matrix  $G$  is given by (31).

$$G = \frac{1}{\rho} B^T K \quad (31)$$

where  $K$  is the solution of control Riccati equation (32).

$$0 = KA + A^T K + C^T C - \frac{1}{\rho} K B B^T K \quad (32)$$

### 3.2 Experimental Setup Description

The experimental setup used in this paper is shown in fig 3.4. Because the frictions are minimized, two wings can be moved up and down freely. However, two wings are highly coupled, the moment of one wing can be affected with another one. For the stability of the setup, a balancing weight  $m_3$  is hanged center of the setup. Widely used and well known block diagram of the experimental setup can be shown as in reference (Butler, 1992). Two wings has the same motor and model of a motor can be described by

$$\frac{\omega}{u} = \frac{K_m}{T_m s + 1}, \text{ where } \omega \text{ is angular velocity. } F_i \text{ is}$$

a lift force causing from motor, and its characteristics is described by  $F_i = C_T \lambda (\omega R)^2 \pi R^2$ , where  $i=1,2$ ,  $C_T$  is lift velocity coefficient,  $\lambda$  is atmospheric density, and  $R$  is each diameter of wing.

### 3.3 System data acquisition

The motor time constant is very small, and the

motors transition condition has a small effect to the entire system. So, through linearization and approximation, the lift force caused by propeller

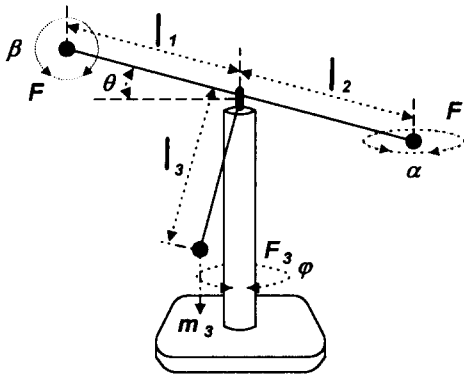


Fig 3.4 Twin rotor MIMO experimental setup

can be represented as

$$F_i \propto \left[ \frac{K_m}{T_m s + 1} \sqrt{U_i} \right]^2 \approx \frac{K_m^2}{2T_m s + 1} u_i \quad i = 1, 2 .$$

Table 3.1 is the setup specification. In the experiment, system coefficients are achieved approximately using system identification method and shown in Table 3.2

Table 3.1 The setup specification

$l_1$	$l_2$	$l_3$	$R_{main}$	$R_{tail}$	$m_3$	$K_m$	$T_m$
24.5cm	28.5cm	25cm	28cm	19cm	22.4g	35.08	0.0043

The DSP board TMS320C31, used in this experiment, has an ability floating point calculation and it has AD/DA port as digital signal processing include digital I/O, counter, timer. TMS320C31 has abilities like 20MIPS ( Million Instruction Per Second) calculation speed, 32bit data bus, internal DMA controller, 64X32 bit instruction cash and so on.

In this experiment we consider two kinds of faults. One is the fault of motor itself. Among the reliable faults of DC motor( Isermann,1993 ), we regards 5% variation of armature resistance as a system faults. Another is the loss of sensor (Encoder) signal. In the first experiment the difference of system behavior or the output waveform couldn't figure out , whether the armature resistance is increased or not, but the fault is detected. In the second experiment we regard the signal loss from each rotor (

main rotor and tail rotor ) during 0.2 and 0.5 second as the system fault .

Table 3.2 Estimated coefficients of the setup

rotator coefficient	main rotor	tail rotor
drift velocity coefficients ( $C_{main}, C_{tail}$ )	$2.18 \times 10^{-6}$	$3.23 \times 10^{-7}$
friction coefficients ( $f_v, f_h$ )	$6.67 \times 10^{-4}$	$6.89 \times 10^{-4}$
inertia coefficients of arms ( $J_v, J_h$ )	$8.33 \times 10^{-4}$	$7.41 \times 10^{-4}$
inertia coefficients of propeller ( $J_{m1}, J_{m2}$ )	$4.12 \times 10^{-7}$	$2.53 \times 10^{-7}$

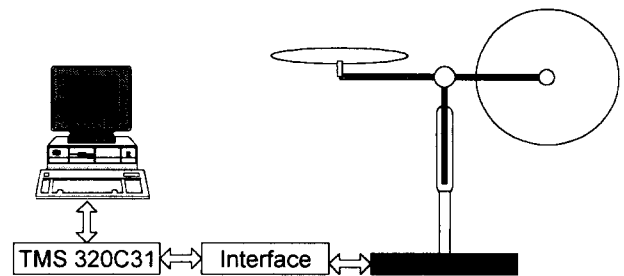


Fig 3.3 Experimental system

#### 4. Experiment Results and Conclusions

Figure 4.2, 4.4, 4.6, 4.8 have shown fault injection experiments data, and figure 4.3, 4.5, 4.7, 4.9 are computer simulation results for the corresponding cases. The rectangular area means that the fault is detected in experiment, and the curve is the simulation results using MatLab, which shows the output behavior of system when the faults are injected. In the experiment, sampling time is taken as 0.05 second, and covariance of input and output noises are taken as  $\sigma_u^2 = 0.03^2$ ,  $\sigma_y^2 = 0.04^2$ , respectively.

The performance of the robust fault detection method for uncertain multivariable systems is exemplified via some experiments in this chapter, and the results are shown below. The key feature of this method is that it accounts for the effects of the variance and bias error due to noise and model mismatch, respectively. The basic algorithm adopted here is robust fault detection method in uncertain multivariable systems which proposed by Kim *et al.*

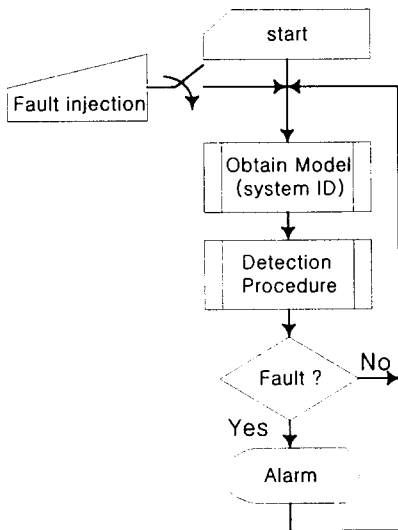


Fig 4.1 Experiment flow chart

(1998) and the experimental result gives the corresponding results. The method depends upon the prior information regarding the nature of the undermodelling and noise. If this information is not available, then it can be estimated from either prior experiments or available data on nonfaulty systems.

Fault detection can be accomplished within 2.5 second (50 steps), which is calculated by the sampling time and can be regard as the detection delay time. For the real application, we must consider about the threshold value and the false alarm probability (Basseville, M., I. Nikiforov (1993)) especially in parametric approach area. In this paper, however, threshold evaluation and false alarm rate evaluation problems are not accomplished yet and will be the further research goal.

### 5. References

Basseville, M., and I. Nikiforov (1993) "*Detection of Abrupt Changes : Theory and Application*". Prentice Hall.  
 Basseville, M. (1988). "Detection of changes in signals and systems - A survey". *Automatica*, **24**, 309-326. Chen,  
 Butler, H. (1992) "*Model Reference Adaptive Control : From theory to practice*." Prentice Hall.  
 Frank, P.M.(1990). "Fault diagnosis in dynamical systems using analytical and knowledge-based redundancy - A survey and some new results", *Automatica* **26**, 459-474, 1990.

Goodwin, G.C. and M.E. Salgado (1989). "A stochastic embedding approach for quantifying uncertainty in the estimation of restricted complexity models." *Int.J.of Adaptive Control and Signal Processing*, **3**, 333-356.  
 Howell, J. (1994), "Model-based fault detection in information poor plants." *Automatica*, **30**, 929-943  
 Isermann, R. (1993 ). "Fault diagnosis of machines via parameter estimation and knowledge processing." *Automatica*, **29**, 815-835.  
 Isermann, R. (1993). "Fault diagnosis of machines via parameter estimation and knowledge processing -Tutorial paper.", *Automatica* **29**, 815-835.  
 Kim, D.W. and O.K. Kwon. (1998) "Robust fault detection method for uncertain multivariable systems." *Trans. KIEE*, Vol.47 No.1 93-98  
 Kwon, O.K., G.C. Goodwin and W.H. Kwon (1994). "Robust fault detection method accounting for modelling errors in uncertain systems." *Control Engineering Practice* **2**, 763-771.  
 Lou, X.C., A.S. Willsky and G.C. Verghese (1986). "Optimally robust redundancy relations for failure detection in uncertain systems." *Automatica*, **22**, 333-344.  
 Makila, P. M. (1990). "Approximation of stable systems by Laguerre filters.", *Automatica* **26**, 333-345.  
 Ninness, B., G.C. Goodwin, O.K. Kwon and B. Carlsson (1991). "Robust fault detection based on low order models." *IFAC Symposium on Fault Detection, Supervision and Safety Technical Processes* Baden-Baden, Sep. 1991. 199-204  
 Patton, R.J., and H. Zhang (1996)."Design of unknown input observer and robust fault detection filters" *Int. J. Control*, **63**, 85-105.  
 Salgado, M.E. (1989). *Issues in Robust identification*. Ph.D. Thesis, University of Newcastle, Australia.  
 Wahlberg, B. (1990). "Robust frequency domain fault detection/diagnosis.", *Proc. of 11th IFAC World Congress*, Tallinn, Estonia, Aug. 1990.

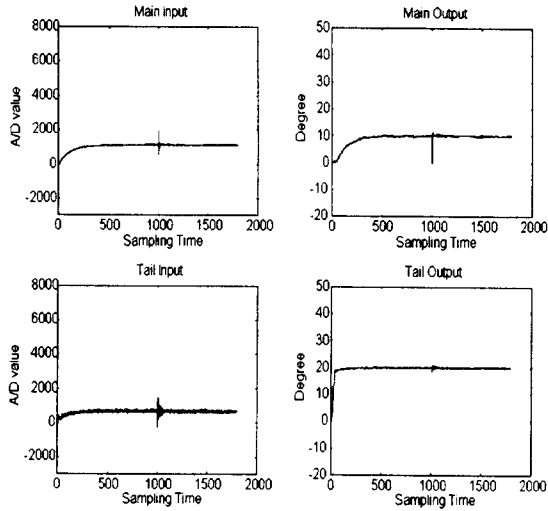


Fig 4.2 Main signal loss for 0.2 sec

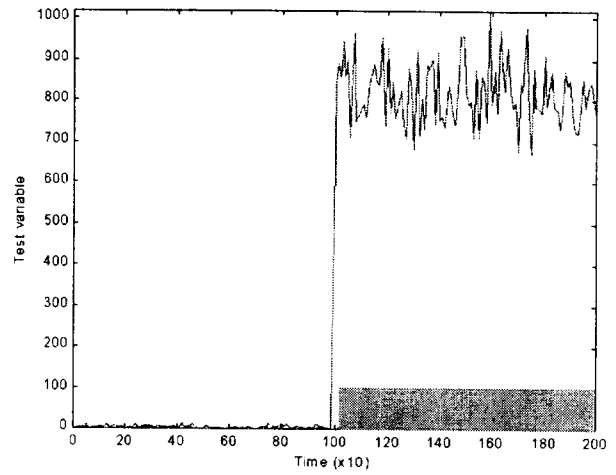


Fig 4.5 Computer simulation and experimental result for the case of fig 4.4

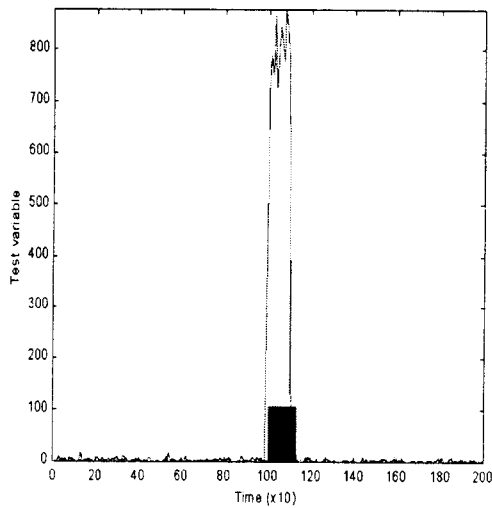


Fig 4.3 Computer simulation and experimental result for the case of fig 4.2

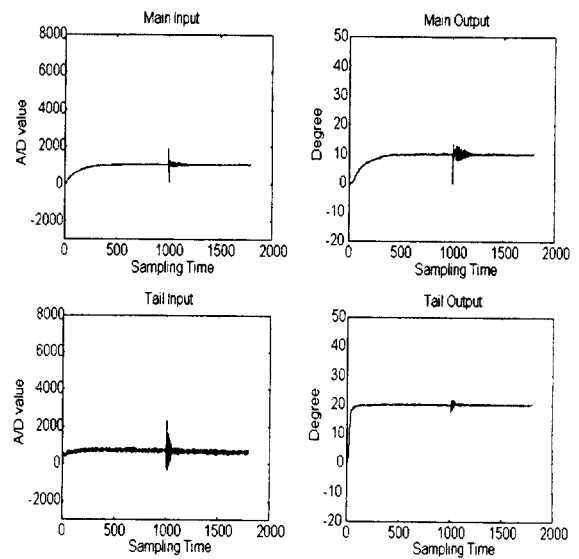


Fig 4.6 Main signal loss for 0.5 sec

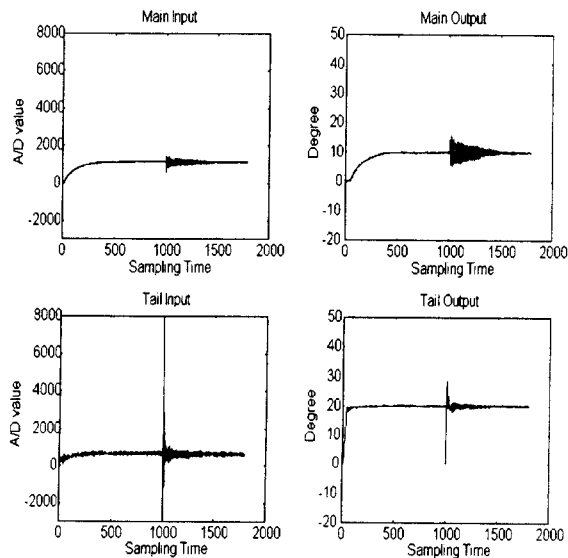


Fig 4.4 Tail signal loss for 0.2 sec

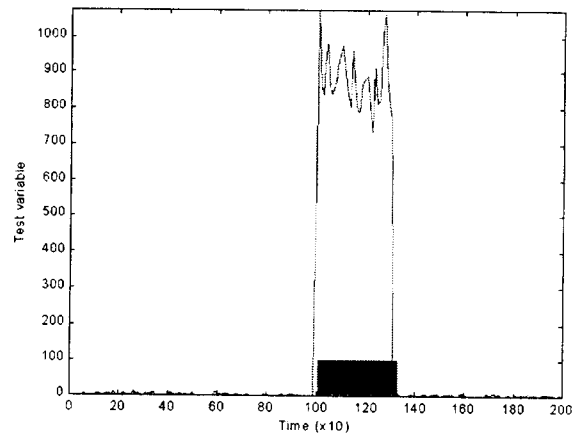


Fig 4.7 Computer simulation and experimental result for the case of fig 4.6



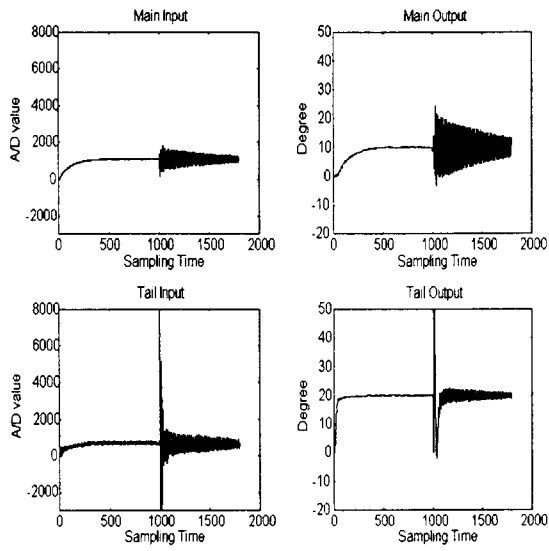


Fig 4.8 Tail signal loss for 0.5 sec

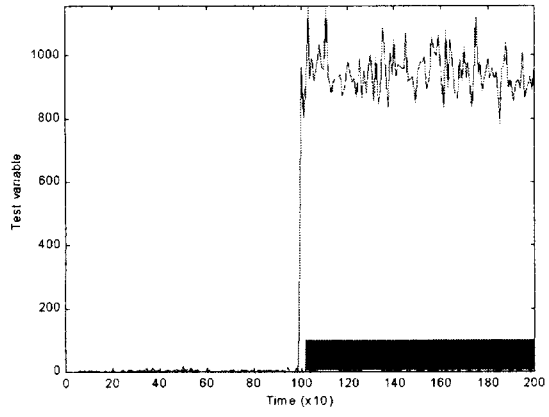


Fig 4.9 Computer simulation and experimental result for the case of fig 4.8

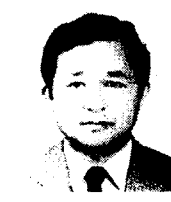
저 자 소 개



**김 대 우(金臺祐)**  
 1963년 2월 12일생. 1988년 인하대 공대 전기공학과 졸업. 1990년 인하대 대학원 전기공학과 졸업(석사). 1990년~1995년 LG산전 연구소 근무. 1995년~1996년 국립공업기술원. 현재 인하대 대학원 전기공학과 박사과정 재학중



**유 호 준(俞浩濤)**  
 1973년 4월 1일생. 1996년 인하대 공대 전기공학과 졸업. 1998년 인하대 대학원 전기공학과 졸업(석사). 현재 인하대 대학원 전기공학과 박사과정 재학중



**권 오 규(權五圭)**  
 1978년 서울대 전기공학과 졸업. 1980년 동 대학원 전기공학과 졸업(석사). 1985년 동 대학원 전기공학과 졸업(공학박사). 1988년~1989년 호주 뉴캐슬대 전기전산공학과 객원교수. 1982년~현재 인하대 전기공학과 교수